



Functional attributes of conifers expanding into temperate semi-arid grasslands modulate carbon and nitrogen fluxes in response to prescribed fire

Justin D. Gay · Bryce Currey ·
Kimberley T. Davis · E. N. Jack Brookshire

Received: 29 January 2024 / Accepted: 1 August 2024 / Published online: 23 August 2024
© The Author(s) 2024

Abstract Fire exclusion is a key factor driving conifer expansion into temperate semi-arid grasslands. However, it remains unclear how reintroducing fire affects the aboveground storage of carbon (C) and nitrogen (N) in the expanding tree species and belowground in soils. To assess the impacts of fire reintroduction C and N pools and fluxes in areas of conifer expansion we targeted a region of the Northern Great Plains that has experienced extensive woody plant expansion (WPE) of two species: ponderosa pine (*Pinus ponderosa*) and juniper (*Juniperus spp.*). We quantified tree mortality of both species to estimate the amount of dead biomass C and N produced by a

recent prescribed fire, in addition to changes in soil C, pyrogenic C (PyC), and N concentrations across a woody-cover gradient using a before/after/control experimental design. Post-fire soil chemical analysis revealed a 2 year increase in mineral soil C, PyC and N, suggesting the return of fire led to the transfer of partially combusted plant organic matter back to the soil. Further, we found that functional trait differences between the two species influenced the distribution of living conifer biomass-N prior to fire. Despite junipers having 41% less total aboveground biomass than ponderosa, they contained two times more aboveground N. Prescribed fire resulted in 88% mortality of all mature juniper stems and increased fire severity correlated with greater pre-fire juniper cover. Ponderosa mortality varied by size class, with >40 cm stem diameter class having only 28% mortality. High mortality and greater aboveground N storage in juniper biomass, compared to ponderosa, led to 77% of the total conifer biomass N lost. Consequently, the functional attributes of expanding trees differentially contribute to fluxes of C and N after the return of fire, with junipers acting as conduits for N movement due to their relatively higher N content in less fire-resistant tissues and ponderosa serving as important and more stable storage pools for C. Together, these findings highlight the importance of considering species-specific traits when planning WPE management strategies at landscape-scales, particularly when goals include C storage or soil nutrient status.

Responsible Editor: Edward Brzostek

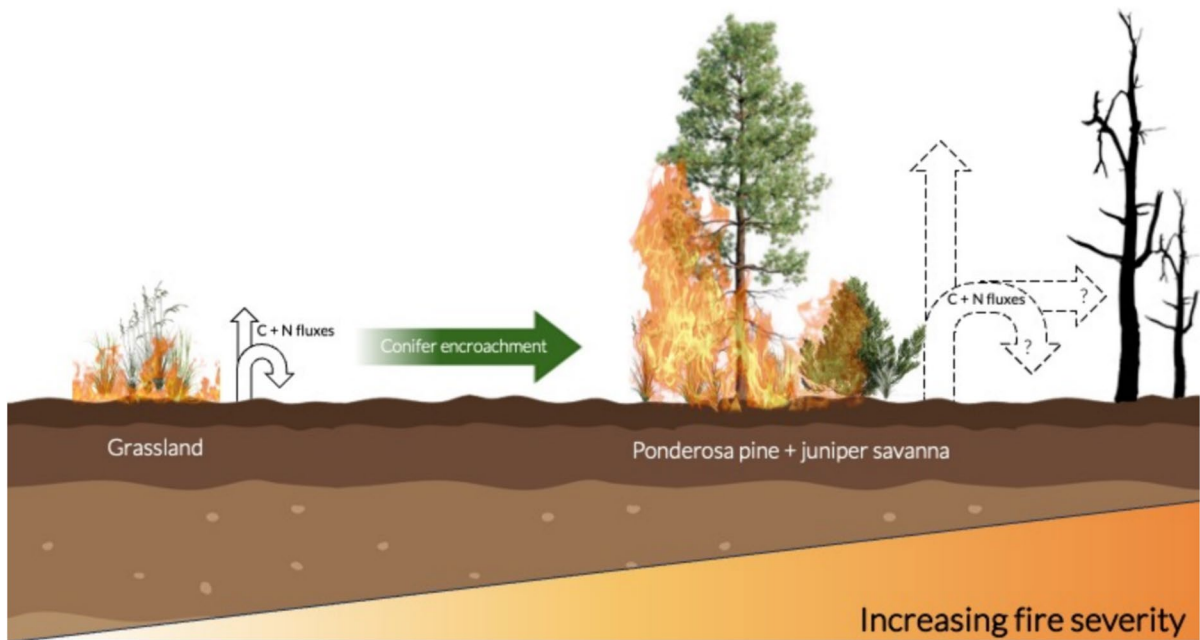
Supplementary Information The online version contains supplementary material available at <https://doi.org/10.1007/s10533-024-01168-6>

J. D. Gay (✉) · B. Currey · E. N. J. Brookshire
Land Resources and Environmental Science, Montana State University, Bozeman, MT 59717, USA
e-mail: Justin.gay@umontana.edu

J. D. Gay · K. T. Davis
USDA Forest Service, Rocky Mountain Research Station,
Missoula Fire Sciences Lab, Missoula, MT 59808, USA

Present Address:

J. D. Gay
Department of Ecosystem and Conservation Sciences,
W.A. Franke College of Forestry and Conservation,
University of Montana, Missoula, MT 59812, USA



The hypothesized effects of how carbon (C) and nitrogen (N) fluxes respond to the return of fire in grasslands experiencing conifer expansion. The question marks represent the input of

fire-altered biomass from conifer trees into the soil and the transformation of living to dead tree biomass which are the focus of this study.

Graphical abstract Keywords Prescribed fire · Woody plant expansion · Nitrogen · Carbon ·

Pyrogenic carbon

Introduction

Woody plant expansion (WPE) into grasslands is a global phenomenon that can drastically alter ecosystem processes such as the cycling of carbon (C) and nutrients critical to primary production and soil organic matter turnover, including nitrogen (N; (Hobbie 1992; Reich et al. 2001; Liao et al. 2008; Barger et al. 2011; González-Roglich et al. 2014). Fire exclusion is a key factor driving conifer expansion in many temperate grasslands (Currey et al. 2022), accelerating WPE, increasing stand density, and replacing grassy understories with bare ground and needle litter (Covington and Sackett 1992). Over decades, the cumulative effects of WPE and fire exclusion transform temperate grassland ecosystems into savanna-grassland mosaics, leading to aboveground accumulation of plant biomass C and N that are susceptible to transformation and loss upon the return of fire (Tilman et al. 2000; MacKenzie et al.

2004). The magnitude of C and N loss in response to fire in areas of recent WPE remain unclear but likely depend on three critical factors: (1) fire severity and frequency, (2) characteristics and quantity of fire-affected vegetation, and (3) direct and indirect fire effects on soil C and N pools. The interactions among these factors are complex as fire not only releases C and N but also generates pyrogenic organic matter (PyOM) from the incomplete combustion of vegetation biomass that contains recalcitrant fractions of C and N (Bird et al. 2015; Torres-Rojas et al. 2020). Thus, PyOM production can mitigate a proportion of C and N losses from volatilization when incorporated into the soil (Santín et al. 2015; Jones et al. 2019), but production estimates are highly dependent on biomass type and formation conditions (Hatton et al. 2016) and have not been previously reported in regions of conifer expansion into temperate grasslands.

Fire exerts a powerful influence over terrestrial biogeochemical cycles as both a catalyst for transformation and vector for loss (McLauchlan et al. 2020; Pausas and Bond 2020). Impacts from fire on ecosystem C and N cycles span different time scales that depend on interactions between fire severity, frequency and the type of vegetation fuel affected. At the most immediate time scale, the combustion of vegetation causes losses of volatilized biomass C and N to the atmosphere that are dependent on the intensity of the burn (Campbell et al. 2007; van der Werf et al. 2017). However, the largest C pool affected by fire often results from the transformation of living C to dead C due to tree mortality, and over time, the decomposition of these trees partially offsets new C inputs from primary production (Meigs et al. 2009; Pellegrini et al. 2023). Historically, many temperate forest ecosystems can accumulate carbon relatively rapidly after fire and shift back to C sinks over decadal timescales, although this process is highly dynamic and depends on fire severity, successful vegetation regeneration and the quantity of remnant coarse woody debris (Bond-Lamberty et al. 2004; Kashian et al. 2006; Dore et al. 2008; Bowman et al. 2009). Conversely, the impact of fire on ecosystem N stocks can be longer lasting as it may take centuries to recover N due to the slow rates of N input processes, especially in dryland ecosystems where biological N fixation inputs may be relatively low (Johnson et al. 1998). While estimates of fire-driven losses of vegetation C (Schuur et al. 2003; Miesel et al. 2018; Adkins et al. 2019; Lasslop et al. 2020) and N (Johnson et al. 1998; Harden et al. 2002; Boby et al. 2010) have been established for some ecosystems, there remains a knowledge gap regarding how vegetation transitions, such as WPE, will affect losses of C and N from the return of fire in temperate semi-arid grasslands.

In contrast to the understanding that fire leads to both immediate and lagged losses of vegetation biomass C and N, effects on mineral soil C and N are more variable and are thought to be largely governed by the severity and/or frequency of fire (Johnson and Curtis 2001; Pellegrini et al. 2018, 2021b). During low to moderate severity fires, mineral soils do not reach sufficiently high temperatures for C and N volatilization, while higher intensity and frequent fire can cause substantial combustion loss (Neary et al. 1999). Responses from single fires can lead to

increases in soil C and N, but these data are more equivocal (Nave et al. 2011; Pellegrini et al. 2018; Johnson and Curtis 2001). Important considerations in examining mechanisms of fire driven increases to mineral soil C and N include understanding how aboveground plant biomass pools are affected by fire, including the fraction that returns to the soil as PyOM.

Quantifying PyOM production rates in temperate grasslands experiencing WPE has yet to be explored but is an important knowledge gap since the shift to more aboveground biomass in WPE areas, likely will increase PyOM production when fire returns. Understanding PyOM accumulation is key for assessing carbon sequestration, as fire transforms plant biomass into PyOM, of which a large fraction is PyC, which can persist in soil for millennia due to its resistance to decomposition (Kuhlbusch 1998; Lehmann et al. 2008). PyOM also alters nutrient availability based on its physiochemical characteristics (Pingree and DeLuca 2017) and contains highly variable concentrations and forms of N that, when present, can be slow to mineralize (Soong and Cotrufo 2015). To date, many estimates of fire C budgets do not account for changes in PyC pools despite the potential for significant inputs (Surawski et al. 2016, Santin et al. 2020, Pellegrini et al. 2021a, b). Understanding whether PyOM accumulates and how woody species differentially contribute to PyC production in encroached grasslands under shifting fire regimes is crucial for predicting long-term C and N dynamics in these non-steady state ecosystems.

To evaluate the impact of fire on C and N storage and fluxes in a semi-arid temperate grassland that has been undergoing conifer expansion, we implemented a large, prescribed fire experiment across a 4,500-hectare area in the northern Great Plains (NGP). Like many temperate drylands this region of the NGP is considered N limited (Hooper and Johnson 1999; Burke et al. 1997; Brookshire et al. 2020), consistent with the low levels of bioavailable-N found in the soils around our study site (Pellegrini et al. 2020). Over the past six decades, this region has witnessed the rapid expansion of *Pinus ponderosa* and *Juniperus scopulorum* (hereafter referred to as ‘ponderosa’ and ‘juniper’ respectively), as documented in previous studies (Wood et al. 2021; Currey

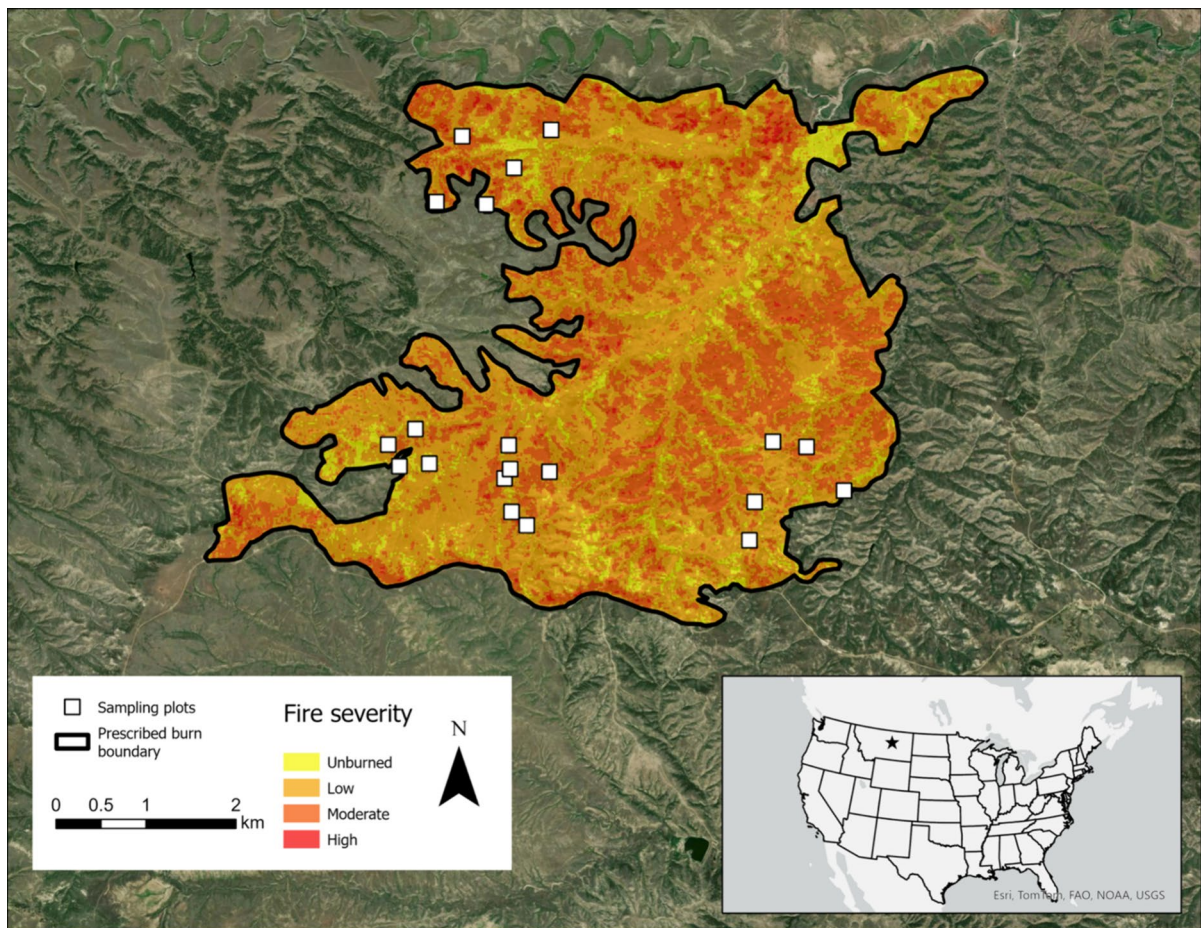


Fig. 1 2018 prescribed burn severity derived using the difference mid-infrared burn spectral index in the Musselshell Missouri River Breaks regions of Central Montana. White squares represent the twenty sampling plots used for this study. Inset

star shows the location of the site within the United States. See Table 1 for binning criteria used to classify burn severity

et al. 2022; Morford et al. 2023). This period of conifer expansion has coincided with a shift in the fire activity. Previously, the area experienced relatively frequent, low-intensity grass fires, but fire suppression and the cessation of Indigenous burning practices have led to less frequent (Umbanhowar 1996) but larger and higher-intensity fires (Reid and Fuhlendorf 2011). The objectives of our study were to: (1) Quantify conifer mortality and associated shifts in living to dead biomass pools of C and N (also referred to as C and N loss in this text) based on the relative mortality of the two dominant tree species, and (2) determine changes in mineral soil C, the PyC fraction of PyOM, and N resulting from fire and WPE.

Materials and methods

Site description

The study area is located in the central Montana region known as the Missouri-Musselshell River breaks (47.436389 N, -108.148333 W) on a 4500-ha block of land managed by the Bureau of Land Management (BLM; Fig. 1.) that is directly adjacent to the Charles M. Russell National Wildlife Refuge area. The mean annual precipitation and temperature across the region is 358 mm and 8.4 °C, respectively. Our study site was unglaciated but intermittently covered by pro-glacial Lake Musselshell during the terminal Pleistocene (Davis et al. 2006). The terrain is

a heterogeneous mix of rolling steppe and hills interspersed with highly eroded escarpments dissected by deep coulees with ephemeral surface water (Fig. S1). Soils are mainly derived from Late Cretaceous Bear Paw Shale, which consists of bedrock with brackish and shallow marine origin and dispersed beds of bentonite clay (Jenson and Varnes 1964). Soils are shallow entisols and vertisols with high clay content and pH ranging from 6.7 in heavily woody areas to 7.1 in grass-dominated areas (Currey 2022).

Between 1958 and 2013 the region experienced extensive WPE at an annual increase of 0.12% tree cover year⁻¹ (Currey et al. 2022). Currently, *Pinus ponderosa* and *Juniperus scopulorum* dominate the woody vegetation, although various *Juniperus* species are present, including *Juniperus horizontalis* and *Juniper communis*, and hybridization is likely. In 2018, prior to the prescribed fire, we established twenty 20×20 m plots that were located >200 m from roads. Plots were established using a stratified random design to capture landscape level variation in tree cover and topography. This resulted in a semi-balanced mix of grass plots (<33% tree canopy cover, n=3), mixed grass-tree plots (33–66% tree canopy cover, n=9), and tree-dominant plots (>66% tree canopy cover, n=8) across a grass-woody gradient. Four out of the 20 plots did not burn during the prescribed fire and were subsequently used as unburned control plots. Topography, edaphic conditions, and vegetation cover of the 4 unburned control plots were similar to the mean conditions of the 16 burned plots (Table SV), prior to fire.

Aboveground biomass and canopy cover estimates

Within each plot, total and species-level tree cover was estimated visually by three of the authors using percent canopy cover and averaged. We tagged and measured the diameter at breast height (DBH; stems >10 cm) and height (H) of all living ponderosa stems (n=631) prior to fire. DBH was then used to calculate basal area (BA). To estimate ponderosa aboveground biomass (AGB) C and N pools, we applied ponderosa-specific allometry using the ponderosa stem measurements from each plot from Tinker et al. 2010:

$$\begin{aligned} \text{Total above ground biomass} &= 0.024 \times (H \times BA) \\ &+ 20.283 + \text{error} \end{aligned} \quad (1)$$

$$\text{Needle biomass} = 0.052 \times BA^{0.982} + \text{error} \quad (2)$$

Variability was estimated following a normal distribution with the mean and standard error calculated from the original estimates from Tinker et al. 2010. To partition biomass pools, needle biomass was subtracted from total aboveground biomass to obtain aboveground woody tissue (e.g., stem, branch, twig) biomass.

To estimate juniper aboveground biomass (AGB), we used an approach based on canopy area (CA) as it is a known strong predictor of AGB across the *Juniperus* genus (Ansley et al. 2012; Cunliffe et al. 2020; Miller et al. 1981; Tiedemann and Klemmedson 2000; Sabin 2008). Although this relationship is not currently known for *Juniperus scopulorum*, the dominant juniper in our study region, we calculated AGB estimates using the average of four other known allometric equations to obtain a genus-level approximation (Table SII). Initially, the relative proportion of juniper and ponderosa CA was recorded and then combined to estimate total tree cover from each plot center. CA estimates for each species were averaged from three observers, who all prior calibrated their visual estimates from an area with established tree cover. After the fire, we returned to the field to calibrate our visual estimates of juniper cover for aboveground biomass allometry calculations in part because juniper canopies are often irregularly shaped and more difficult to estimate compared to ponderosa.

To do this, we used an area footprint (0.04 ha) in locations outside our plots to visually estimate juniper cover, as outlined above, and then compared it to an area derived from crown measurements of all junipers within the plot footprint. We repeated this process 10 times for a total of 102 juniper crown areas measured. Ocular estimates tended to linearly underestimate measured CA by 33±2% (Fig. S3). Therefore, initial CA estimates were adjusted based on a correction factor derived from the field calibration measurements. To partition biomass pools into aboveground wood and needle we used the relationship in Ansley et al. 2012.

Prescribed fire management and fire severity assessment

On May 3, 2018, the BLM implemented a large, prescribed burn across the study area using a combination of ground teams with drip torches and aerial ignition. Prior to the fire, weather conditions were stable with average windspeeds of 11–13 km per hour across the course of the day. Surface temperatures ranged from 20 to 23 °C and relative humidity remained <35% throughout the day. Weather conditions were recorded with a belt weather kit and Kestral weather meter. The lowest dead fuel moistures were 5% for unshaded areas and 8% for shaded areas. The prescribed fire was ignited at 8:50 AM, had peak fire activity between 13:00 and 14:15 and managed until 18:30. Fire activity significantly decreased starting at 14:15 when the smoke column laid down over the burn area and active smoldering was observed into the next day. BLM field observations on May 14th noted open timber stands with stem char heights up to 2 and 3 m and greater burn activity in stands with greater juniper understory. All plots were visited two weeks after the fire to assess evidence of burning.

To determine the fire severity of the prescribed fire, we calculated the difference Mid-Infrared Burn Index (dMIRBI) spectral index within the fire perimeter obtained from the MTBS national database (<https://www.mtbs.gov>). The dMIRBI spectral index has been used in other savanna ecosystems (Trigg and Flasse 2001; Tran et al. 2018) and has been shown to successfully detect changes in soil properties post-fire (Fernández et al. 2021). Spectral indices were calculated using pre- and post-fire images of the study area from the Sentinel-2 satellite provided by the European Space Agency (acquired via Google Earth Engine). The Mid-Infrared Burn Index (MIRBI) was calculated using short-wave infrared band 1 (B11) and short-wave infrared band d (B12) using the following equation:

$$MIRBI = 10 \times B11 - 9.8 \times B12 \quad (3)$$

The burn severity index was calculated by subtracting the MIRBI pre-fire from the MIRBI post-fire using Eq. 4 and is on a 0–1 scale.

$$dMIRBI = MIRBI_{Pre-Fire} - MIRBI_{Post-Fire} \quad (4)$$

Table 1 Severity classification and % area affected in the 2018 prescribed fire unit

Classification	dMIRBI index	% Area of burn unit
Unburned	<0.14	9
Level 1 (low)	0.14–0.36	59
Level 2 (moderate)	0.36–0.60	31
Level 3 (high)	>0.60	1

Severity was measured using the Difference Mid-infrared Burn Index (dMIRBI) spectral index acquired from the Sentinel-2 satellite

The unburned zone cutoff was defined by the highest dMIRBI index observed across the four control plots

To assess the fire severity within the study area, we developed a relative classification system by dividing the burn index into four severity levels that were based off of the mean dMIRBI of the four unburned control plots (Fernández et al. 2021). Level 1 was unburned, Level 2 experienced low severity, Level 3 experienced moderate severity, and Level 4 experienced high severity (Table 1).

Tree mortality assessment and dead C and N biomass pool estimates

To assess tree mortality, plots were re-surveyed for living stems in May 2018, two weeks after the prescribed fire had been conducted. For each tree, the percentage of crown volume scorch was visually estimated by foliar necrosis. Stem mortality for both species was assigned if >70% of the crown was scorched 8/7/2024 8:42:00 AM. In May 2019 trees were resurveyed to validate the initial mortality assessment by ensuring no crown regrowth. Plot level tree mortality is reported as a percentage of trees killed based on the pre-fire living stem count.

To calculate the fractional species-specific contributions to the dead C biomass pools, we multiplied the plot-level mortality by each of the structural biomass pools (e.g., canopy needle and stem biomass) within each of the 16 plots that burned. We applied the same approach to calculate the production of dead N biomass pools since volatilization temperatures for C and N are similar (200 °C). This approach is similar to the widely-used “consumed biomass approach” that assumes all C from burned aboveground biomass is emitted

(Andreae and Merlet 2001; van der Werf et al. 2010; Wiedinmyer et al. 2011). However, we use the terminology “live or dead biomass C or N” because fire-induced tree mortality and the resulting pool of dead wood biomass is often the largest fire driven C transformation in conifer ecosystems (Meigs et al. 2009).

Soil, surface PyOM, and woody tissue collection, processing, and chemical analysis

Pre-fire mineral soil samples were collected to a 10 cm depth in April 2018 across the 20 established plots. Post-fire soil samples were collected to the same depth in May 2018, June 2018, May 2019 and June 2019. Soil sampling was designed to capture the cover classification of the plot (e.g., tree, grass-tree mix and grass). In tree plots, we sampled areas underneath individual tree canopies of each conifer species and in plots with less cover we collected a greater proportion of soil samples under grass cover. Samples were collected on slopes $<25^\circ$ and >1 m from the base of tree stems. In total, five samples were taken from each plot and then composited to a single representative sample in the field. Soil samples were taken with a 2 cm diameter soil probe (Oakfield Apparatus). In total, we collected 500 individual soils samples that were composited by plot for a total of 100 composited soil samples that were analyzed. Twenty plots were used for C and N analyses and 12 plots were used for PyC analysis based on the availability of paired pre-fire soil samples. All soils were oven-dried at 105°C until a constant mass was reached, and then milled to a fine powder for 12 h in stainless steel jars on a slow-rolling tumbler. To calculate elemental soil pools, three soil bulk density cores were extracted from each plot at a 0–10 cm mineral soil depth using a 5 cm diameter slide hammer. Bulk density cores were composited and dried at 105°C for 48 h before being sieved at <2 mm. To convert C, PyC, and N concentrations to a mass per unit area (Mg ha^{-1}), concentrations were multiplied by each plot's sampled bulk density and soil depth (10 cm). Mineral soil bulk density ranged from 0.71 to 1.11 g cm^{-3} and had a mean of 0.90 g cm^{-3} . We collected surface charred organic matter post-fire from 10 randomly selected plots to determine C and N concentrations of consumed surface fuels. To determine C and N concentrations

of foliar biomass, we collected and aggregated sunlit needles from the canopies of three ponderosa pine and junipers in each of five randomly selected plots. Ponderosa foliar samples were collected from similarly aged trees in the upper canopy using a shotgun. Sunlit juniper foliar samples were collected by hand-clipping. Woody biomass C and N concentrations were determined from tree cores and cross-sections of five randomly selected ponderosa and juniper. Entire ponderosa tree cores and juniper cross sections (sap and heart wood) were ground using a rotary mill. Needles were dried at 60°C for 48 h and then hand milled in liquid. Both foliar and woody tissue were sent to Agvise Laboratories (Northwood, ND) for chemical analysis.

To determine total C and N concentrations of the soil, needle and woody biomass, and post-fire surface char, we used the dry combustion method. Soils and post-fire surface char were analyzed at Montana State University's Environmental Analytical Laboratory with a Costech ESC 4010 elemental analyzer and Truspec CN analyzer (LECO, St Joseph, MI, USA), respectively. PyOM covers a broad spectrum of fire derived organic material and in this study we quantify the PyC fraction by using the peroxide-weak nitric acid digestion protocol (Kurth et al. 2006). Briefly, replicate soil samples (~ 1.0 g) from each pre- and post-fire plot were individually added to a solution of 30% H_2O_2 and 1 M HNO_3 and heated to 100°C for 16 h. Samples were then visually inspected for evidence of any further reaction (i.e., effervescence) and allowed to react until effervescence subsided. Upon digestion completion, samples were filtered through a Whatman #2 filter, dried, and ground with mortar and pestle. Samples were then massed in aluminum tins for dry combustion. Duplicates were run for 10% of samples to ensure analytical precision, which we defined to be $<10\%$ for PyC, C and N.

Statistical analysis

We used ordinary least squares (OLS) linear regression to determine differences in woody cover (%) between treatment and control plots, prior to fire. To assess fire-induced conifer mortality, we calculated species- and stem diameter size-class specific mortality rates. We also assessed how fire severity (dMIRBI) varied with species composition by using OLS linear regression to model fire severity

as a function of ponderosa and juniper cover. To determine conifer biomass C and N loss we used Welch's two sample *t* tests to compare pre- and post-fire biomass C and N estimates for each species. To understand how total C and N loss varied with pre-fire species composition, we used OLS linear regression to model losses as a function of pre-fire ponderosa or juniper cover, for each species individually (Table SII). All simple linear models were assessed for normally distributed residuals.

To evaluate fire driven changes to soil elemental concentrations we used linear mixed effects model using the lme4 package in R (Bates et al. 2015) with the fixed effect of treatment that contains four categorical levels pre-burn, post-burn, pre-control, and post-control and a random effect for plot to account for repeated soil measurements over time. To evaluate if treatment(s) in both OLS and linear mixed effects models accounted for variation in response variables, we performed a type II ANOVA using the 'anova' function in the lmerTest package (Kuznetsova et al. 2017), and post-hoc comparisons were made using pairwise Tukey HSD. Soil chemistry results are reported as estimated marginal means (emmeans package; Lenth 2021). To understand how soil chemistry was impacted by the interaction of fire and tree cover we used linear models to assess change (post-fire concentration—pre-fire concentration) as a function of pre-fire mature stem density. All model residuals were evaluated for normality. The only model requiring a log-transformation of the response variable to conform to a normal distribution was for soil nitrate concentration (Table SV). Treatment significance was set a priori to $\alpha=0.05$. For linear regression model summary output see Table SII and T-test model summary output in Table SIII. All statistical analyses were conducted in R version 4.1.1 (R Core team, 2021).

Results

Fire severity, tree mortality, C and N biomass loss

Prior to fire, average juniper coverage across all plots was $20 \pm 3\%$ while ponderosa was $39 \pm 6\%$. Grass coverage in the plots ranged from 5 to 75% with an average $28 \pm 5.7\%$. There were no differences in total

tree cover between the unburned controls ($52 \pm 12\%$) and burned plots ($60 \pm 6\%$; $p=0.52$) before the fire.

Aerial imagery analysis and the dMIRBI index indicated that majority of the fire was classified as low-moderate burn severity (Fig. 1). Nine percent of the unit was unburned, 59% experienced low fire severity, 31% moderate fire severity, and $<1\%$ experienced high fire severity (Table 1). Overall prescribed burning was effective at reducing total aboveground woody biomass as we observed a $35 \pm 6\%$ mean mortality rate for all living stems >10 cm DBH and 98% of all saplings were killed by fire within our plots (Fig S4). Higher pre-fire ponderosa plot cover was associated with lower burn severity (Fig. 2b; $p=0.05$), while plots with higher pre-fire juniper cover were associated with greater burn severity (Fig. 2b; $p=0.07$). Tree mortality was disproportionately driven by the $88 \pm 5\%$ mean mortality rate of juniper stems. Ponderosa was more resistant to fire with a $37 \pm 5\%$ mean decrease in living stems (Fig. 2a). In plots that burned at a low severity, 39% of ponderosa stems in the 10–20 cm DBH class were killed while only 18% of stems with >40 cm DBH were killed (Fig. 3). In plots that burned at a moderate severity 75% of 10–20 cm DBH stems were killed while 66% of stems with a >40 cm DBH were killed, although low counts of large trees ($n=3$) and less total area burned at moderate severity influence these summaries (Table 1; Fig. 3). We generally observed higher survival rates of ponderosa among larger diameter trees, although this trend was most pronounced in plots that experienced low-severity fire.

Pre-fire, 42.8 ± 8.4 Mg C ha⁻¹ was stored in aboveground tree biomass, with a greater fraction stored in ponderosa compared to juniper ($p=0.05$, Table 2). Using the mean value from the sixteen plots that burned, we estimate that 50% (21.7 ± 8.4 Mg C ha⁻¹) of total aboveground woody plant biomass-C was lost due to tree mortality with similar losses from each species 11.7 Mg C ha⁻¹ from juniper and 10.07 Mg C ha⁻¹ from ponderosa ($p=0.72$; Fig. 6). Before the fire, 306 ± 44 kg N ha⁻¹ was stored in tree biomass, with a disproportionate amount stored in juniper compared to ponderosa ($p<0.002$) We estimate that 78% (238 kg N ha⁻¹; Fig. 6) of living conifer biomass N was lost with a greater proportion coming from juniper compared to ponderosa ($p<0.002$). Total N and C losses increased with total pre-fire tree cover ($p<0.069$, $p=0.015$, respectively (Fig S5)) and in

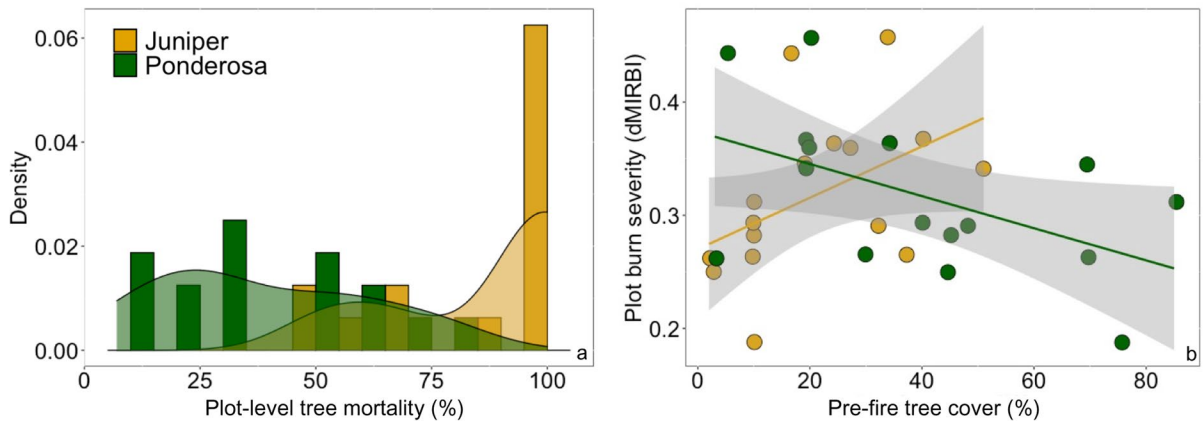


Fig. 2 Distribution of tree mortality percentages by plot with color indicating tree species. Yellow represents *Juniperus spp.*, and green represents *Pinus ponderosa*. **a** Linear relationship

between plot burn severity using the difference mid-infrared burn index (dMIRBI) and pre-fire percent total tree cover. **b** Gray area in **b** represents the 95% confidence interval

Fig. 3 Relative fire driven mortality of *Pinus ponderosa* stems by diameter at breast height size classes (DBH). Note difference in y-axis scale of stem counts by size class

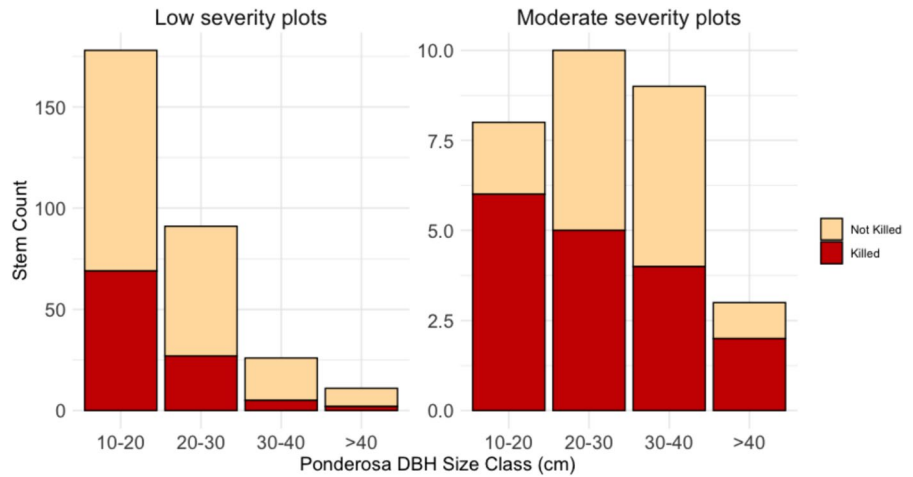


Table 2 Tree biomass elemental concentrations and mean pre-fire aboveground tree biomass (AGB) carbon (C) and nitrogen (N) pools (kg ha^{-1}) across the 16 plots that burned

	C conc. (%)	N conc. (%)	C:N	AGB C Pool	AGB N Pool
<i>Juniperus spp</i>					
Wood	50.1 ± 0.43	0.10 ± 0.02	506	6290 ± 1090	13.1 ± 2.0
Needle	51.4 ± 0.44	1.07 ± 0.10	49	9640 ± 1650	200 ± 28
<i>Pinus ponderosa</i>					
Wood	51.2 ± 1.5	0.03 ± 0.01	2290	23,000 ± 4980	12.6 ± 2.0
Needle	49.3 ± 0.30	1.02 ± 0.19	50	3880 ± 677	80.5 ± 12
Total tree AGB				42,800 ± 8400	306 ± 44

Values are means ± standard error

Tree totals are the sums of the individual needle and wood combined

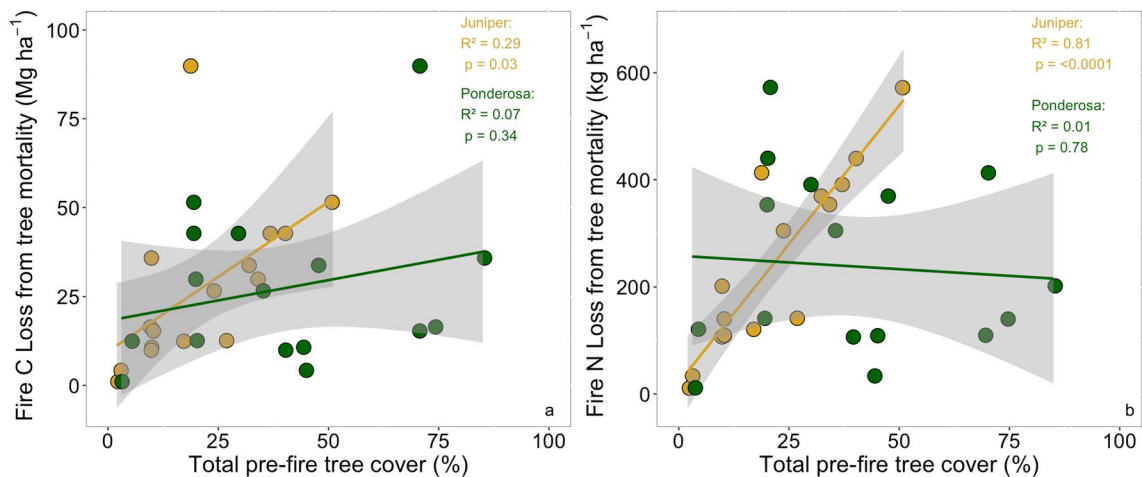


Fig. 4 Linear relationships between pre-fire tree cover and carbon (C) loss (**a**) and nitrogen (N) loss from mortality (**b**). Colors indicate species where yellow is *Juniperus spp* and

green is *Pinus ponderosa*. Grey shaded area represents the 95% confidence interval. Note the difference in area scaled units on the y-axis

plots with greater pre-fire juniper cover ($p = < 0.0001$, $p = 0.03$, respectively). This linear relationship with juniper C and N loss can be used to extrapolate across a juniper cover gradient in similar regions of the northern Great Plains experiencing WPE: for every 1% increase in juniper cover 12.8 kg N ha⁻¹ and 2.85 Mg C ha⁻¹ are lost due to fire (Fig. 4). In contrast, there was no relationship in N and C losses with pre-fire ponderosa cover ($p = 0.78$, $p = 0.34$, respectively, Fig. 4).

Fire driven changes in soil chemistry

Concentrations of mineral soil (0–10 cm depth) C and N increased by 32% and 23% after fire in plots that burned (Fig. 5, Table SII), while C and N in unburned plots did not change ($p = 0.22$ and $p = 0.25$, respectively). Total soil C pools increased ($p = 0.001$, Table SI) after fire by roughly 4 Mg C ha⁻¹ from 13.3 ± 1.2 to 17.7 ± 1.2 Mg C ha⁻¹ and soil N pools increased ($p = 0.002$) by 210 kg N ha⁻¹ from 1000 ± 60 to 1210 ± 50 kg N ha⁻¹. There was suggestive evidence that soil C:N ratios increased ($p = 0.06$, Fig. 5). Changes in soil chemistry before and after fire were partially explained by tree expansion as increases in soil C and N were associated with pre-fire mature stem density cover ($p = 0.05$ and $p = 0.03$).

Soil PyC concentrations increased ($p = 0.002$) by 42% from 0.33 ± 0.03 pre-fire to 0.47 ± 0.04

post-fire which equates to an area scaled increase of 1.2 ± 0.3 Mg PyC ha⁻¹. Despite the increase in soil PyC, the relative proportion of PyC to total soil carbon was not affected by fire ($23 \pm 0.01\%$; $p = 0.39$). The mean concentration of C and N in the post-fire surface char samples were $20\% \pm 4.0$ and $0.77\% \pm 0.13$, respectively. The mean C: N ratio of the surface char was 27 ± 3.0 . We found little statistical evidence of WPE related predictors (mature stem density, % woody cover, % mortality) affecting PyC production (Table SII).

Discussion

Differential conifer resistance to fire drives variability in fire severity and C and N fluxes

Overall, prescribed burning was effective at reducing total aboveground woody biomass and fire severity was strongly influenced by the pre-fire woody cover. Specifically, an increase in juniper cover was associated with higher fire severity, while a higher proportion of ponderosa cover led to reduced fire severity. These findings indicate that different woody species play a significant role in how grasslands respond to the reintroduction of fire in the northern Great Plains subjected to WPE management. The

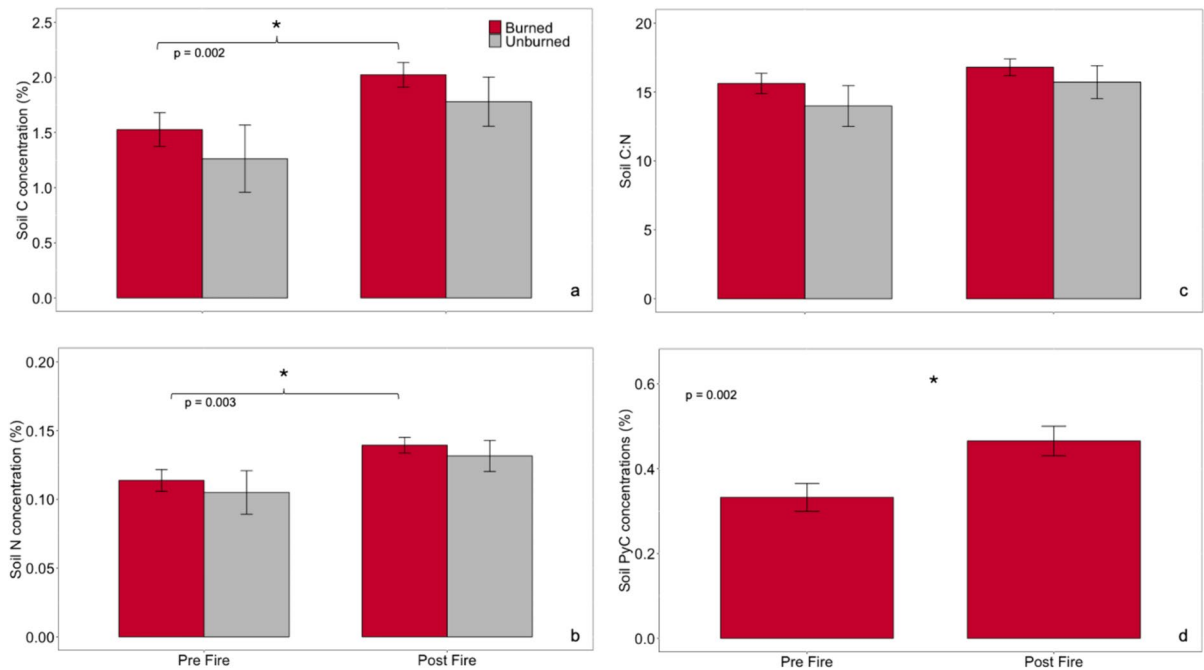


Fig. 5 Differences between pre-and post-fire soil carbon (a), nitrogen (b), soil C:N (c), and pyrogenic carbon (PyC) (d) at 0–10 cm soil depth. Grey bars represent the unburned control plots. Values shown are estimated marginal means and stand-

ard error based on the linear mixed affect models. *denotes significance from Tukey’s honest significant difference for panels a and b while d is from analysis of variance ($\alpha=0.05$)

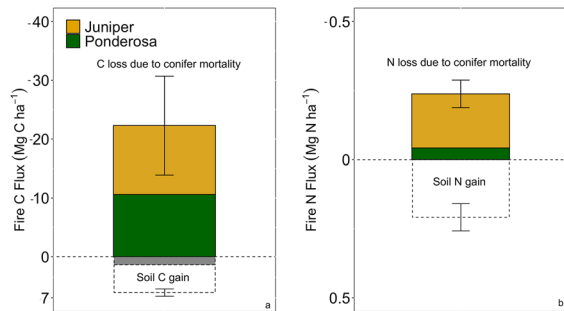


Fig. 6 Area-scaled carbon (C) and nitrogen (N) flux estimates from the plots that burned in the 2018 prescribed fire, in grids (a) and (b), respectively. Loss estimates are shown as negative based on the transition from living aboveground conifer biomass to dead biomass and the unknown fraction that was volatilized. The grey shaded area in (a) indicates the proportion of soil pyrogenic carbon (PyC) gain relative to total soil C gain. Error bars represent \pm standard error of the total above and belowground flux

continued proliferation of juniper in these ecosystems may lead to increased fire severity due to their flammability and low and brushy stature.

The relative composition of woody species was identified as a key factor affecting C and N losses. Importantly, we found that (1) ponderosa and juniper mortality equally contributed to C losses despite far greater mortality of juniper, (2) pre-fire juniper cover predicted N losses, and (3) juniper biomass had 3 times the aboveground N content of ponderosa, and this, which combined with the twofold greater juniper mortality indicated that pre-fire juniper cover and mortality was predictive of potential N loss. The shift in ecosystem structure towards larger and older ponderosa trees creates a more stable aboveground carbon storage environment, supporting the findings of Lutz et al. (2018). Notably, ponderosa C losses were similar to those of juniper, despite 48% less mortality, indicating a significant C loss per ponderosa stem relationship, regardless of stem diameter.

Differences in each species’ morphology explains their contrasting responses to low-moderate intensity fires. Mature ponderosa trees are highly resistant to low intensity fires due to their thick bark, open crown, and branching pattern (Fitzgerald 2005). In contrast,

junipers, with their thin bark, compact crown, and highly volatile resin content, are less resistant to fire (Scher 2002). In addition to being less resistant to fire, juniper stored a disproportionately higher amount of aboveground N before the fire, despite having 41% less total aboveground biomass compared to ponderosa. Moreover, the location of N storage in both species influenced potential N losses due to fire, with juniper having a higher ratio of foliar to woody N (15:1 versus 6:1, on a per mass basis kg N ha^{-1}) and three times the wood N content compared to ponderosa (Table 2). These observations suggest that junipers play a significant role in facilitating the movement of N during fires, primarily because they store a higher amount of N in less fire-resistant structures. Based on our estimations, juniper contributed to approximately 78% of (Fig. 6) the total live tree N lost from fire.

We calculated total losses of $22.3 \text{ Mg C ha}^{-1}$ and 238 kg N ha^{-1} (Fig. 6) in conifer biomass due to tree mortality caused by fire. The C loss estimate far exceed aboveground C stocks in grasslands near the site in this study ($\sim 0.5 \text{ Mg C ha}^{-1}$, Brookshire, unpublished data). This highlights that the increased C accumulation across the landscape from WPE leads enhanced C loss upon the return of fire. Accurate estimation of C losses due to fire is difficult as there are initial volatile emission losses followed by a period of gradual release of C from dead-biomass decomposition. Therefore, using tree mortality as a proxy for potential losses represents a conservative approach since the largest C transformation from fire is often tree mortality. Nevertheless, these fire driven C fluxes oppose the steady input of C from annual net primary productivity and if we assume the roughly $1 \text{ Mg C ha yr}^{-1}$ mean growth rate from the previous 63 years (Currey 2022), we estimate that it would take roughly 20 years to sequester the C lost from conifer mortality. This approach to understand the C balance does not account for the complexity of C fluxes during post-fire regrowth and compensatory effects from non-tree productivity (Wirth et al. 2002). Our N loss estimates are within the range (106–414 kg N ha) of studies in other dry conifer forests (Johnson et al. 1998). It is important to emphasize that many of these prior studies have primarily concentrated on N losses in forest floor and surface soil, neglecting the large pool of N affected by the mortality of trees. It is important to note that these C and N loss estimates

reflect the mean 60% tree cover of the burned plots, coverage that is likely higher than other shrub and rangelands of the northern Great Plains, but reflective of other encroached areas in the region.

Mineral surface soil N increases offset biomass N losses while C losses were only partially buffered by soil C increases

After decades of fire suppression, a single and low-moderate severity prescribed fire led to an increase in mineral soil C and N. We posit that the increase in total soil C was largely driven by C inputs from less thermally altered plant biomass that was not quantified as PyC in our chemical analysis. We find support for this hypothesis through the high C and N concentrations in the surface char produced by the fire. If we assume a 0.36 cm layer of char and ash was produced, a bulk density of 0.62 g cm^3 —values which were estimated from a similar lower intensity wildfire in a pine scrubland (Cerdà and Doerr 2008) and the 20% C concentration from surface PyOM in this study, this equates to an increase of 4.5 Mg C ha^{-1} that could have been incorporated into the mineral layer post-fire, an estimate that exceeds the empirical results from this study of an increase of 4 Mg C ha^{-1} . It is important to note that ash bulk density and production can vary significantly between ecosystems and fire intensities, as well as between different locations within the same fire (Bodí et al. 2014). Moreover, a recent experimental study found that the highest inputs of PyOM-C from forest fuel types are those with higher proportions of woody to fine fuels (Santin et al. 2020) which is further support that the PyOM production from the incomplete combustion of woody conifer biomass across our sites is partially responsible for the increases in total mineral soil C.

Additionally, we observed increases in mineral soil N. Importantly, the increases in soil N are roughly equivalent to the estimated living loss of N from conifer mortality (Fig. 6). Fire is an important nutrient recycling pathway in many semi-arid systems (McLauchlan et al. 2020; Pausas and Bond 2020) and the substantial input of N to soil from conifer combustion may help improve the low nutrient status found in the surface soils across our study area (Table SIII). Increasing tree cover in

grasslands has the potential to redistribute nutrients from the topsoil to slow turnover biomass pools in woody tissue. Thus, fire may help remediate an amplifying feedback between WPE and progressive soil nutrient limitation. The increase in soil N after fire is within the range of a previous meta-analysis (Johnson and Curtis 2001) and very similar to the 27% increase reported by (Klopatek 1991) beneath burned junipers in a pinyon-juniper woodland. In a global meta-analysis, Pellegrini et al (2018) found that lower severity fire was associated with total soil N increases in needleleaf forests—likely due to the smoldering of organic matter in the thick organic horizon of these ecosystems. Thus, we suspect that the smoldering of ground litter and the incorporation of incompletely combusted living tissue from conifers into the soil largely contributed to the increase in soil N. Our findings contrast with previous research in our study area which showed that recurrent fire substantially reduced surface soil C and N pools and soil enzyme activity, compared to unburned areas. This reduction was in part due to sustained decreases in conifer litter input (Pellegrini et al. 2020) and the shallower depth of soil samples. Comparing these differing results highlights the need to better understand the threshold at which low severity prescribed burns transition from driving soil C and N loss to promoting soil C and N accumulation, across. Additionally, it underscores the need to explore how climate conditions impact ecosystem productivity and vegetation dynamics during the intervals between burn periods.

Prescribed fire produces a large quantity of a highly stable form of soil C in conifer encroached temperate semi-arid grasslands

We find that a single, low-moderate intensity fire led to the production of 1.2 Mg ha^{-1} of PyC in the mineral layer and represents a large fraction (23%) of the total soil C increase that we observed (Fig. 6). Our estimate of $1.2 \text{ Mg PyC ha}^{-1}$ is lower than what was produced in the organic soil layer of another prescribed fire study in a more productive ponderosa pine-Douglas-fir forest in western Montana ($2.2 \text{ Mg PyC ha}^{-1}$; DeLuca et al. 2020). However, it is important to highlight that observed increases of PyC in this study occurred in the mineral layer where

PyC is relatively protected from surface mobilization relative to the organic layer, and can therefore persist for long periods of time (Abiven & Santín, 2019; Rumpel 2015). It is possible that the short-term vertical transportation of PyC from the organic layer into the mineral layer may have been driven by the integration of the fine ($<2 \text{ mm}$) PyC fraction via the temporary formation of cracks in the vertic soils found across the study site (Rumpel 2015). Thus, the time of year when fire occurs, and underlying soil factors may play a role in the stabilization of PyC in mineral soil depths. Our PyC processing methods captured only the $<2 \text{ mm}$ chemical fraction and excluded charcoal fragments $>2 \text{ mm}$ which can account for upwards of 50% of the visibly detected charcoal (Nocentini et al. 2010). This suggests that the overall production of PyC was likely larger than we detected, but we would need additional chemical, thermal and observational methods to quantify the full PyC spectrum.

The production of PyC in a WPE affected grassland buffered against C loss by roughly 6%. This estimate of PyC production falls within the range of previous estimates of tree biomass to PyC conversion percentages in coniferous forests (1% to 20%; Tinker and Knight 2000; Lynch et al. 2004; Preston and Schmidt 2006). Despite the increases in PyC across the landscape, the proportion of PyC to total soil C did not change after fire. This either suggests that a fraction of surface mineral soil C was volatilized or that our method of PyC determination likely captured only a fraction of the PyC added to the soil. While there are numerous methods to quantify PyC as it exists across a spectrum of thermally altered PyOM material (Bird et al. 2015) it remains an important uncertainty in ecosystem C budgets.

Future research directions

Our experimental results provide new understanding of how fire reintroduction affects C and N fluxes in a grassland experiencing conifer expansion. However, further work is needed to partition C and N losses determined by the completeness of decomposition of burnt C and N biomass, combustion emission losses, as well as the relative contributions of burned herbaceous biomass and the litter pool underneath woody canopies. Another outstanding question that remains is how the newly incorporated PyOM

will influence and respond to future soil C and N processes (e.g., C and N mineralization) in WPE affected grasslands.

Grassland ecosystems have historically relied on frequent fire to support nutrient cycling and productivity. Consequently, the suppression of fire across North American grasslands has led to the reduction of PyC inputs, impacting soil physical processes, microbial activity, and nutrient cycling (Gao et al. 2024). Therefore, while the return of fire may be critical to restoring the role PyC plays in soil nutrient cycling processes in WPE affected grasslands, the interaction of trees as a new source material of PyC may alter soil ecosystem function. One important factor to consider is the higher C:N ratio of woody material compared to herbaceous material. The mean C:N ratio of the PyOM from this study (28) is higher than the stoichiometric threshold that governs net N mineralization versus immobilization (20–25; (Manzoni et al. 2008; Mooshammer et al. 2014). This suggests that despite increases in biologically available N immediately post-fire (Table SIII), C rich PyOM fluxes to soils could transiently depress N mineralization rates, and possibly affect future plant availability of N. However, few studies have focused on how woody PyOM may affect soil nutrient cycling in natural grassland settings where there is more plant community complexity and low background external N inputs. The most relevant study was conducted in Western Montana, where the authors evaluated the effects of conifer wood biochar (i.e., PyOM) addition to acidic grassland soils. They report subtle outcomes, including C conservation, organic N retention, and increased plant available inorganic N (Gao and DeLuca 2020). Indeed, both the intensity of fire and source material can influence short- and long-term soil C and N processes (Gundale and DeLuca 2006; Deluca et al 2015). Thus, in grasslands undergoing WPE an important area of inquiry is determining the environmental conditions under which PyOM addition stimulate or reduce soil N mineralization, nitrification, and immobilization and how tree species and fire intensity modulate these patterns over time.

Lastly, more work is needed to understand how herbaceous communities, particularly non-native forbs and grasses, will respond to changes in nutrient availability following prescribed fire treatments in areas affected by WPE in the northern Great Plains.

Conclusions

Our findings emphasize the strong influence of plant community composition on C and N fluxes following a single prescribed fire. The combustion of juniper significantly affects N fluxes, driven by the high relative contribution to aboveground N storage, elevated foliar to total biomass N ratio, high wood N content, and heightened susceptibility to combustion. Thus, one consideration for the reintroduction of fire into semi-arid temperate grasslands experiencing WPE is the possibility of juniper driven fire N-losses redirecting the ecosystem towards an alternative ecosystem state. However, despite this long-term theoretical possibility, we observed that the increase in surface soil N stocks after fire nearly offsets estimated N losses from total tree mortality. This suggests the possibility of using prescribed fire to reintroduce biomass-immobilized N back to the soil, after long periods of fire absence.

Additionally, our results have implications for ecosystem C balance. Lower severity fires in WPE prone areas promotes greater survival of larger ponderosa trees, thereby shifting ecosystem structure and C storage towards larger and older trees. Furthermore, we observe increases in soil PyC indicating that a significant fraction of aboveground biomass consumed in the fire was thermally transformed and redistributed back to soils. While the exact functional properties and long-term fate of PyC are still poorly understood, PyC generally enhances ecosystem soil C persistence and can improve nutrient retention. Consequently, increased frequency of prescribed fires to manage WPE may promote ecosystem C sequestration over time in these cool semi-arid environments, facilitated by slow overall decomposition and the gradual accumulation and burial of PyC. Together, these findings underscore the importance of considering species-specific traits when planning fire management strategies at ecosystem-scales, particularly when goals include C storage or soil nutrient status.

Acknowledgements The authors would like to thank two anonymous reviewers for their suggestions. Additionally, we thank Matt Comer for his insights and guidance in establishing the field plots, coordination of the prescribed burn, and general knowledge of the region. We gratefully acknowledge Tory Dille, Evan Bilbrey, Ryan Malmquist, Hannah Duff, and Shealyn Malone for assistance with field sample collection and processing. Justin Gay (USDA affiliation) was an ORISE (Oak

Ridge Institute for Science and Education) Fellow and not a U.S. Department of Agriculture employee.

Author contributions Justin Gay, Jack Brookshire and Bryce Currey conceived the project and established the field plots. Justin Gay and Bryce Currey processed field samples. Justin Gay and Bryce Currey analyzed the data with interpretation assistance from Jack Brookshire and Kimberley Davis. Justin Gay, Bryce Currey and Kimberley Davis created data visualizations. Justin Gay drafted the initial manuscript. All co-authors revised, read, and approved the final manuscript.

Funding This research was supported by grants from the U.S. Bureau of Land Management (agreement numbers L16AS00082 and L21AS00472), the Murdock Trust (Reference number 201812566), and the U.S. National Science Foundation (Award Number OIA-1632810).

Data availability The data that support the findings of this study are available in the public open access data repository Dryad and available here: <https://doi.org/10.5061/dryad.v9s4mw756>

Declarations

Conflict of interest The authors declare that they have no conflict of interest.

Open Access This article is licensed under a Creative Commons Attribution 4.0 International License, which permits use, sharing, adaptation, distribution and reproduction in any medium or format, as long as you give appropriate credit to the original author(s) and the source, provide a link to the Creative Commons licence, and indicate if changes were made. The images or other third party material in this article are included in the article's Creative Commons licence, unless indicated otherwise in a credit line to the material. If material is not included in the article's Creative Commons licence and your intended use is not permitted by statutory regulation or exceeds the permitted use, you will need to obtain permission directly from the copyright holder. To view a copy of this licence, visit <http://creativecommons.org/licenses/by/4.0/>.

References

- Abiven S, Santín C (2019) Editorial: from fires to oceans: dynamics of fire-derived organic matter in terrestrial and aquatic ecosystems. *Front Earth Sci* 7:31
- Adkins J, Sanderman J, Miesel J (2019) Soil carbon pools and fluxes vary across a burn severity gradient three years after wildfire in Sierra Nevada mixed-conifer forest. *Geoderma* 333:10–22. <https://doi.org/10.1016/j.geoderma.2018.07.009>
- Andreae MO, Merlet P (2001) Emission of trace gases and aerosols from biomass burning. *Global Biogeochem Cycles* 15:955–966. <https://doi.org/10.1029/2000G B001382>
- Ansley RJ, Mirik M, Surber BW, Park SC (2012) Canopy area and aboveground mass of individual redberry juniper (*Juniperus pinchotii*) trees. *Rangel Ecol Manage* 65:189–195. <https://doi.org/10.2111/REM-D-11-00112.1>
- Barger NN, Archer SR, Campbell JL et al (2011) Woody plant proliferation in North American drylands: a synthesis of impacts on ecosystem carbon balance. *J Geophys Res Biogeosci*. <https://doi.org/10.1029/2010JG001506>
- Bates D, Mchler M, Bolker B, Walker S (2015) Fitting linear mixed-effects models using lme4. *J Stat Softw* 67(1):1–48. <https://doi.org/10.18637/jss.v067.i01>
- Bird MI, Wynn JG, Saiz G et al (2015) The pyrogenic carbon cycle. *Annu Rev Earth Planet Sci* 43:273–298. <https://doi.org/10.1146/annurev-earth-060614-105038>
- Boby LA, Schuur EAG, Mack MC et al (2010) Quantifying fire severity, carbon, and nitrogen emissions in Alaska's boreal forest. *Ecol Appl* 20:1633–1647. <https://doi.org/10.1890/08-2295.1>
- Bodí MB, Martin DA, Balfour VN et al (2014) Wildland fire ash: production, composition and eco-hydro-geomorphic effects. *Earth Sci Rev* 130:103–127. <https://doi.org/10.1016/j.earscirev.2013.12.007>
- Bond-Lamberty B, Wang C, Gower ST (2004) Net primary production and net ecosystem production of a boreal black spruce wildfire chronosequence. *Glob Change Biol* 10:473–487. <https://doi.org/10.1111/j.1529-8817.2003.0742.x>
- Bowman DMJS, Balch JK, Artaxo P et al (2009) Fire in the Earth system. *Science* 324:481–484
- Brookshire ENJ, Stoy PC, Currey B, Finney B (2020) The greening of the northern Great Plains and its biogeochemical precursors. *Glob Change Biol* 26:5404–5413. <https://doi.org/10.1111/gcb.15115>
- Burke IC, Lauenroth WK, Parton WJ (1997) Regional and temporal variation in net primary production and nitrogen mineralization in Grasslands. *Ecology* 78:1330–1340. [https://doi.org/10.1890/0012-9658\(1997\)078\[1330:RATVIN\]2.0.CO;2](https://doi.org/10.1890/0012-9658(1997)078[1330:RATVIN]2.0.CO;2)
- Campbell J, Donato D, Azuma D, Law B (2007) Pyrogenic carbon emission from a large wildfire in Oregon, United States. *J Geophys Res Biogeosci*. <https://doi.org/10.1029/2007JG000451>
- Cerdà A, Doerr SH (2008) The effect of ash and needle cover on surface runoff and erosion in the immediate post-fire period. *CATENA* 74:256–263. <https://doi.org/10.1016/j.catena.2008.03.010>
- Covington WW, Sackett SS (1992) Soil mineral nitrogen changes following prescribed burning in ponderosa pine. *Forest Ecol Manage* 54:175–191. [https://doi.org/10.1016/0378-1127\(92\)90011-W](https://doi.org/10.1016/0378-1127(92)90011-W)
- Cunliffe AM, McIntire CD, Boschetti F et al (2020) Allometric relationships for predicting aboveground biomass and sapwood area of oneseed juniper (*Juniperus monosperma*) trees. *Front Plant Sci* 11:94
- Currey, B (2022) Woody plant expansion in the northern Great Plains: a multi-scale assessment of the drivers and the ecological implications of increasing woody abundance in a temperate open ecosystem. Dissertation, Montana State University.
- Currey B, McWethy DB, Fox NR, Brookshire ENJ (2022) Large contribution of woody plant expansion to recent

- vegetative greening of the northern Great Plains. *J Biogeogr* 49:1443–1454. <https://doi.org/10.1111/jbi.14391>
- Davis NK, Locke WW, Pierce KL, Finkel RC (2006) Glacial Lake Musselshell: late Wisconsin slackwater on the Laurentide ice margin in central Montana, USA. *Geomorphology* 75:330–345. <https://doi.org/10.1016/j.geomorph.2005.07.021>
- DeLuca TH, Gundale MJ, MacKenzie MD, Jones DL (2015) Biochar effects on soil nutrient transformations. In: Lehmann J, Joseph S (eds) *Biochar for environmental management*. Routledge, London, pp 421–454
- DeLuca TH, Gundale MJ, Brimmer RJ, Gao S (2020) Pyrogenic carbon generation from fire and forest restoration treatments. *Front for Glob Change*. <https://doi.org/10.3389/ffgc.2020.00024>
- Dore S, Kolb TE, Montes-Helu M et al (2008) Long-term impact of a stand-replacing fire on ecosystem CO₂ exchange of a ponderosa pine forest. *Glob Change Biol* 14:1801–1820. <https://doi.org/10.1111/j.1365-2486.2008.01613.x>
- Fernández C, Fernández-Alonso JM, Vega JA et al (2021) Exploring the use of spectral indices to assess alterations in soil properties in pine stands affected by crown fire in Spain. *Fire Ecol* 17:2. <https://doi.org/10.1186/s42408-020-00089-7>
- Fitzgerald Stephen A (2005) Fire ecology of ponderosa pine and the rebuilding of fire-resilient ponderosa pine ecosystems. In: Ritchie Martin W., Maguire Douglas A., Youngblood Andrew Tech Coordinators. *Proceedings of the Symposium on Ponderosa Pine: Issues, Trends, and Management, 2004 October 18–21, Klamath Falls, OR*. Gen. Tech. Rep PSW-GTR-198. Albany, CA: Pacific Southwest Research Station, Forest Service, U.S. Department of Agriculture: 197–225
- Gao S, DeLuca TH (2020) Biochar alters nitrogen and phosphorus dynamics in a western rangeland ecosystem. *Soil Biol Biochem* 148:107868. <https://doi.org/10.1016/j.soilbio.2020.107868>
- Gao S, Eisenberg C, Morford SL, DeLuca TH (2024) Fire exclusion, pyrogenic carbon, and ecosystem function: what have we lost? *Anthropocene* 46:100438. <https://doi.org/10.1016/j.ancene.2024.100438>
- González-Roglich M, Swenson JJ, Jobbágy EG, Jackson RB (2014) Shifting carbon pools along a plant cover gradient in woody encroached savannas of central Argentina. *Forest Ecol Manage* 331:71–78. <https://doi.org/10.1016/j.foreco.2014.07.035>
- Gundale MJ, DeLuca TH (2006) Temperature and source material influence ecological attributes of ponderosa pine and Douglas-fir charcoal. *Forest Ecol Manage* 231:86–93. <https://doi.org/10.1016/j.foreco.2006.05.004>
- Harden JW, Mack M, Veldhuis H, Gower ST (2002) Fire dynamics and implications for nitrogen cycling in boreal forests. *J Geophys Res Atmos*. <https://doi.org/10.1029/2001JD000494>
- Hatton P-J, Chatterjee S, Filley TR et al (2016) Tree taxa and pyrolysis temperature interact to control the efficacy of pyrogenic organic matter formation. *Biogeochemistry* 130:103–116. <https://doi.org/10.1007/s10533-016-0245-1>
- Hobbie SE (1992) Effects of plant species on nutrient cycling. *Trends Ecol Evol* 7:336–339. [https://doi.org/10.1016/0169-5347\(92\)90126-V](https://doi.org/10.1016/0169-5347(92)90126-V)
- Hooper DU, Johnson L (1999) Nitrogen limitation in dryland ecosystems: responses to geographical and temporal variation in precipitation. *Biogeochemistry* 46:247–293. <https://doi.org/10.1007/BF01007582>
- Jenson FS, Varnes HD (1964) *Geology of the Fort Peck area, Garfield, McCone, and Valley Counties, Montana*. USGS, Virginia
- Johnson DW, Curtis PS (2001) Effects of forest management on soil C and N storage: meta analysis. *Forest Ecol Manage* 140:227–238. [https://doi.org/10.1016/S0378-1127\(00\)00282-6](https://doi.org/10.1016/S0378-1127(00)00282-6)
- Johnson DW, Susfalk RB, Dahlgren RA, Klopatek JM (1998) Fire is more important than water for nitrogen fluxes in semi-arid forests. *Environ Sci Policy* 1:79–86. [https://doi.org/10.1016/S1462-9011\(98\)00008-2](https://doi.org/10.1016/S1462-9011(98)00008-2)
- Jones MW, Santín C, van der Werf GR, Doerr SH (2019) Global fire emissions buffered by the production of pyrogenic carbon. *Nat Geosci* 12:742–747. <https://doi.org/10.1038/s41561-019-0403-x>
- Kashian DM, Romme WH, Tinker DB et al (2006) Carbon storage on landscapes with stand-replacing fires. *Bioscience* 56:598–606. [https://doi.org/10.1641/0006-3568\(2006\)56\[598:CSOLWS\]2.0.CO;2](https://doi.org/10.1641/0006-3568(2006)56[598:CSOLWS]2.0.CO;2)
- Klopatek J (1991) Fire effects on carbon and nitrogen pools of woodland floor materials and soils in a pinyon-juniper forest ecosystem. *Fire and the Environment*
- Kuhlbusch TAJ (1998) Black carbon and the carbon cycle. *Science* 280:1903–1904. <https://doi.org/10.1126/science.280.5371.1903>
- Kurth VJ, MacKenzie MD, DeLuca TH (2006) Estimating charcoal content in forest mineral soils. *Geoderma* 137:135–139. <https://doi.org/10.1016/j.geoderma.2006.08.003>
- Kuznetsova A, Brockhoff PB, Christensen RHB (2017) lmerTest package: tests in linear mixed effects models. *J Stat Softw* 82(13):1–26. <https://doi.org/10.18637/jss.v082.i13>
- Lasslop G, Hantson S, Harrison SP et al (2020) Global ecosystems and fire: multi-model assessment of fire-induced tree-cover and carbon storage reduction. *Glob Change Biol* 26:5027–5041. <https://doi.org/10.1111/gcb.15160>
- Lehmann J, Skjemstad J, Sohi S et al (2008) Australian climate–carbon cycle feedback reduced by soil black carbon. *Nature Geosci* 1:832–835. <https://doi.org/10.1038/ngeo358>
- Lenth, R. (2021). emmeans: estimated marginal means, aka least-squares means (R package version 1.6.2-1) [Computer software]. <https://CRAN.R-project.org/package=emmeans>
- Liao C, Peng R, Luo Y et al (2008) Altered ecosystem carbon and nitrogen cycles by plant invasion: a meta-analysis. *New Phytol* 177:706–714. <https://doi.org/10.1111/j.1469-8137.2007.02290.x>
- Lutz JA, Furniss TJ, Johnson DJ et al (2018) Global importance of large-diameter trees. *Glob Ecol Biogeogr* 27:849–864. <https://doi.org/10.1111/geb.12747>
- Lynch JA, Clark JS, Stocks BJ (2004) Charcoal production, dispersal, and deposition from the Fort Providence experimental fire: interpreting fire regimes from charcoal

- records in boreal forests. *Can J for Res* 34:1642–1656. <https://doi.org/10.1139/x04-071>
- MacKenzie MD, DeLuca TH, Sala A (2004) Forest structure and organic horizon analysis along a fire chronosequence in the low elevation forests of western Montana. *For Ecol Manage* 203:331–343. <https://doi.org/10.1016/j.foreco.2004.08.003>
- Manzoni S, Jackson RB, Trofymow JA, Porporato A (2008) The global stoichiometry of litter nitrogen mineralization. *Science* 321:684–686. <https://doi.org/10.1126/science.1159792>
- McLauchlan KK, Higuera PE, Miesel J et al (2020) Fire as a fundamental ecological process: research advances and frontiers. *J Ecol* 108:2047–2069. <https://doi.org/10.1111/1365-2745.13403>
- Meigs GW, Donato DC, Campbell JL et al (2009) Forest fire impacts on carbon uptake, storage, and emission: the role of burn severity in the eastern Cascades, Oregon. *Ecosystems* 12:1246–1267. <https://doi.org/10.1007/s10021-009-9285-x>
- Miesel J, Reiner A, Ewell C et al (2018) Quantifying changes in total and pyrogenic carbon stocks across fire severity gradients using active wildfire incidents. *Front Earth Sci*. <https://doi.org/10.3389/feart.2018.00041>
- Miller, E. L., Meeuwig, R. O., and Budy, J. D. (1981). Biomass of Singleleaf Pinyon and Utah Juniper (No. Research Paper INT-273). United States Department of Agriculture, Forest Service, Intermountain Forest and Range Experimental Station.
- Mooshammer M, Wanek W, Hämmerle I et al (2014) Adjustment of microbial nitrogen use efficiency to carbon:nitrogen imbalances regulates soil nitrogen cycling. *Nat Commun* 5:3694. <https://doi.org/10.1038/ncomms4694>
- Morford SL, Allred BW, Jensen ER et al (2023) Mapping tree cover expansion in Montana, U.S.A. rangelands using high-resolution historical aerial imagery. *Remote Sens Ecol Conserv*. <https://doi.org/10.1002/rse2.357>
- Nave LE, Vance ED, Swanston CW, Curtis PS (2011) Fire effects on temperate forest soil C and N storage. *Ecol Appl* 21:1189–1201. <https://doi.org/10.1890/10-0660.1>
- Nearly DG, Klopatek CC, DeBano LF, Ffolliott PF (1999) Fire effects on belowground sustainability: a review and synthesis. *For Ecol Manage* 122:51–71. [https://doi.org/10.1016/S0378-1127\(99\)00032-8](https://doi.org/10.1016/S0378-1127(99)00032-8)
- Nocentini C, Certini G, Knicker H et al (2010) Nature and reactivity of charcoal produced and added to soil during wildfire are particle-size dependent. *Org Geochem* 41:682–689. <https://doi.org/10.1016/j.orggeochem.2010.03.010>
- Pausas JG, Bond WJ (2020) On the three major recycling pathways in terrestrial ecosystems. *Trends Ecol Evol* 35:767–775. <https://doi.org/10.1016/j.tree.2020.04.004>
- Pellegrini AFA, Ahlström A, Hobbie SE et al (2018) Fire frequency drives decadal changes in soil carbon and nitrogen and ecosystem productivity. *Nature* 553:194–198. <https://doi.org/10.1038/nature24668>
- Pellegrini AFA, Hobbie SE, Reich PB et al (2020) Repeated fire shifts carbon and nitrogen cycling by changing plant inputs and soil decomposition across ecosystems. *Ecol Monogr* 90:e01409. <https://doi.org/10.1002/ecm.1409>
- Pellegrini AFA, Caprio AC, Georgiou K et al (2021a) Low-intensity frequent fires in coniferous forests transform soil organic matter in ways that may offset ecosystem carbon losses. *Glob Change Biol* 27:3810–3823. <https://doi.org/10.1111/gcb.15648>
- Pellegrini AFA, Harden J, Georgiou K et al (2021b) Fire effects on the persistence of soil organic matter and long-term carbon storage. *Nat Geosci*. <https://doi.org/10.1038/s41561-021-00867-1>
- Pellegrini AFA, Reich PB, Hobbie SE et al (2023) Soil carbon storage capacity of drylands under altered fire regimes. *Nat Clim Chang* 13:1089–1094. <https://doi.org/10.1038/s41558-023-01800-7>
- Pingree MRA, DeLuca TH (2017) Function of wildfire-deposited pyrogenic carbon in terrestrial ecosystems. *Front Environ Sci*. <https://doi.org/10.3389/feenvs.2017.00053>
- Preston CM, Schmidt MWI (2006) Black (pyrogenic) carbon: a synthesis of current knowledge and uncertainties with special consideration of boreal regions. *Biogeosciences* 3:397–420. <https://doi.org/10.5194/bg-3-397-2006>
- R Core Team (2021) R: A language and environment for statistical computing. R Foundation for Statistical Computing. <https://www.R-project.org>
- Reich PB, Peterson DW, Wedin DA, Wrage K (2001) Fire and vegetation effects on productivity and nitrogen cycling across a forest-grassland continuum. *Ecology* 82:1703–1719. [https://doi.org/10.1890/0012-9658\(2001\)082\[1703:FAVEOP\]2.0.CO;2](https://doi.org/10.1890/0012-9658(2001)082[1703:FAVEOP]2.0.CO;2)
- Reid AM, Fuhlendorf SD (2011) Fire management in the national wildlife refuge system: a case study of the Charles M. Russell national wildlife refuge. *Montana Rala* 33:17–23. <https://doi.org/10.2111/1551-501X-33.2.17>
- Rumpel C (2015) Movement of biochar in the environment. In: Lehmann J, Joseph S (eds) *Biochar for environmental management: science, technology and implementation*. Routledge, London
- Sabin, B. S. (2008). Relationship between allometric variables and biomass in western juniper (*Juniperus occidentalis*) (Thesis).
- Santín C, Doerr SH, Preston CM, González-Rodríguez G (2015) Pyrogenic organic matter production from wildfires: a missing sink in the global carbon cycle. *Glob Change Biol* 21:1621–1633. <https://doi.org/10.1111/gcb.12800>
- Santín C, Doerr SH, Jones MW et al (2020) The relevance of pyrogenic carbon for carbon budgets from fires: insights from the FIREX experiment. *Global Biogeochem Cycles* 34:e2020GB006647. <https://doi.org/10.1029/2020GB006647>
- Scher JS (2002) *Juniperus scopulorum*. In: Fire effects information system [Online].
- Schuur EAG, Trumbore SE, Mack MC, Harden JW (2003) Isotopic composition of carbon dioxide from a boreal forest fire: inferring carbon loss from measurements and modeling. *Global Biogeochem Cycles*. <https://doi.org/10.1029/2001GB001840>
- Soong JL, Cotrufo MF (2015) Annual burning of a tallgrass prairie inhibits C and N cycling in soil, increasing recalcitrant pyrogenic organic matter storage while reducing N availability. *Glob Change Biol* 21:2321–2333. <https://doi.org/10.1111/gcb.12832>

- Surawski NC, Sullivan AL, Roxburgh SH et al (2016) Incorrect interpretation of carbon mass balance biases global vegetation fire emission estimates. *Nat Commun* 7:11536. <https://doi.org/10.1038/ncomms11536>
- Tiedemann AR, Klemmedson JO (2000) Biomass and nutrient distribution and system nutrient budget for western juniper in central Oregon. *Northwest Sci* 74(1):12–24
- Tilman D, Reich P, Phillips H et al (2000) Fire suppression and ecosystem carbon storage. *Ecology* 81:2680–2685. [https://doi.org/10.1890/0012-9658\(2000\)081\[2680:FSAECS\]2.0.CO;2](https://doi.org/10.1890/0012-9658(2000)081[2680:FSAECS]2.0.CO;2)
- Tinker DB, Knight DH (2000) Coarse woody debris following fire and logging in Wyoming Lodgepole pine forests. *Ecosystems* 3:472–483. <https://doi.org/10.1007/s100210000041>
- Tinker D, Stakes GK, Arcano RM (2010) Allometric equation development, biomass, and aboveground productivity in Ponderosa Pine Forests, Black Hills, Wyoming. *West J Appl for* 25:112–119. <https://doi.org/10.1093/wjaf/25.3.112>
- Torres-Rojas D, Hestrin R, Solomon D et al (2020) Nitrogen speciation and transformations in fire-derived organic matter. *Geochim Cosmochim Acta* 276:170–185. <https://doi.org/10.1016/j.gca.2020.02.034>
- Tran BN, Tanase MA, Bennett LT, Aponte C (2018) Evaluation of spectral indices for assessing fire severity in Australian temperate forests. *Remote Sens* 10:1680. <https://doi.org/10.3390/rs10111680>
- Trigg S, Flasse S (2001) An evaluation of different bi-spectral spaces for discriminating burned shrub-savannah. *Int J Remote Sens* 22:2641–2647. <https://doi.org/10.1080/01431160110053185>
- Umbanhowar CE (1996) Recent fire history of the northern Great Plains. *Am Midl Nat* 135:115–121. <https://doi.org/10.2307/2426877>
- van der Werf GR, Randerson JT, Giglio L et al (2010) Global fire emissions and the contribution of deforestation, savanna, forest, agricultural, and peat fires (1997–2009). *Atmos Chem Phys* 10:11707–11735. <https://doi.org/10.5194/acp-10-11707-2010>
- van der Werf GR, Randerson JT, Giglio L et al (2017) Global fire emissions estimates during 1997–2016. *Earth Syst Sci Data* 9:697–720. <https://doi.org/10.5194/essd-9-697-2017>
- Wiedinmyer C, Akagi SK, Yokelson RJ et al (2011) The Fire INventory from NCAR (FINN): a high resolution global model to estimate the emissions from open burning. *Geosci Model Dev* 4:625–641. <https://doi.org/10.5194/gmd-4-625-2011>
- Wirth C, Czimczik CI, Schulze E-D (2002) Beyond annual budgets: carbon flux at different temporal scales in fire-prone Siberian Scots pine forests. *Tellus b Chem Phys Meteorol* 54:611–630. <https://doi.org/10.3402/tellusb.v54i5.16690>
- Wood DJA, Powell S, Stoy PC et al (2021) Is the grass always greener? Land surface phenology reveals differences in peak and season-long vegetation productivity responses to climate and management. *Ecol Evol* 11:11168–11199. <https://doi.org/10.1002/ece3.7904>

Publisher's Note Springer Nature remains neutral with regard to jurisdictional claims in published maps and institutional affiliations.